Ministry of National Education and Scientific Research

University of Craiova

Faculty of Automation, Computers and Electronics

Ph.D. Thesis

Features Extraction Techniques for Medical Images Diagnosis and Retrieval

A thesis submitted in partial fulfillment of the requirements for the degree of

Doctor of Philosophy in Computer Science and Information Technology,

University of CRAIOVA, Romania

Author:
FAIQ SABBAR BAJI

Supervisor:
Prof. Dr. Ing.
MIHAI LUCIAN MOCANU

Craiova, 2018

Abstract

With the popularity of the network and expansion of multimedia technology, the traditional techniques of information retrieval do not meet the user requirements any more. Recently, the medical images retrieval and diagnosis based on the contents of the image (color, texture, and shape have become the hot topic to satisfy a great development. In this thesis, new methods are proposed for the retrieval and diagnosis of medical images. The first method proposed is to solve the problem of regions of interest (ROI) based on the image retrieval. The ROI technique, which is based on segmenting the image into fixed partitions, is computationally costly. The proposed method is based on the connected components and object of interest to generate the histogram and statistical texture feature vectors. These resulted vectors are used to retrieve images from a large image database. The color and texture features of the connected components are computed from the histograms of the quantized HSV (hue, saturation, value) color space and Gray Level Co-occurrence Matrix (GLCM), respectively. The vectors matching process is based on the histogram intersection. It is obvious that the experimental data clearly shows the efficiency of the proposed method in comparison to the traditional ROI technique in terms of computational cost.

A variety of techniques have been developed for image recuperation and medical image diagnosis by use content of texture features. Texture features proved a robust tool to analysis the local feature of a texture and are widely adopted in image retrieval and medical image diagnosis. In this research, we try to make efficient the LBP method by suggest a new variant of the LBP feature, the so-called Local Ternary Patterns (LTP) for detecting mid sagittal plane (MSP) in brain slices and a new addition for CBIR called uniform extended local ternary pattern (UELTP).

Shape representation is an essentially issue in shape recognition and computer vision. Shape representation has been used in many applications of CBIR. This research is concerned with the problems of the images are frequently obtained from a huge database dedicated for images; this retrieval by apply the contour of an object. Chain Code Histogram (CCH) is applying to create a feature vector which is used to characterize a given shape;

Brain tumor detection and analysis are important issue for medical image processing due to the complexity of images. Since the growth of tumors causes asymmetry in the affected parts of the brain, the proposed method calculates asymmetry based on the intensity difference between the two sides of a mid-sagittal plane (MSP). One of the problems of this method appears when the brain object is rotated or tilted. A new method is proposed to solve this problem, by determining mid-sagittal plane in slice of type T1-weighted images, based on low intensity of the inter-hemispheric fissure (IF) region. In this research, is performed using K-means clustering algorithm for image segmentation of the brain MRI image and connected component label to determine the location and size of the tumor. The experimental result clearly shows the efficiency of the proposed method in comparison to the traditional systems in terms of computational cost and consumed time.

Contents

Chapter 1: Introduction

1.1 Introduction

The content based image retrieval (CBIR) technique is used to retrieval of images from a huge database depending on content of three-primary features: color, texture, and shape recognition. The majority of the CBIR techniques extract content based features from the image query and database image, and apply the comparison between both images in order to identify the variances among their features in terms of their spatial distance function [1] [2]. Commercial image retrieval systems mostly use keywords or text with each image for the process of retrieval. That is the reason why they are called Text Based Image Retrieval (TBIR). A good example of that would be Google Images [3]. The issue can be summed up as follows: the search results are completely contingent on the keywords used to describe the image. Additionally, it is almost impossible to search images that lack such keywords or descriptions [4].

The image searching and retrieving based on content of texture characteristic can be achieved through various methods developed. These techniques are constructed according to the comparison of the values obtained from query and target images, also known as second-order method. It is used for computing the measurements image texture features such as coarseness, directionality, moments and GLCM. In this thesis, proposes new methods for image retrieval, based on local texture features. These techniques can be implemented in various applications, such as medical diagnosis [5]. The Local Binary Pattern (LBP) [6] is a robust tool to characterize the local feature of a texture. Numerous of the applications of LBP include face recognition, analysis of facial expressions, texture classification, and background modeling [7].

Shape recognition is a primary issue feature in CBIR [8]. The shape of objects plays an important role to discriminant the visual information.. The shape descriptor of an object feature has more influence than other features (such as color and texture) and it is strongly tied to the object functionality or identity. However, the processes of perceptual shape features and measuring the similarity between the shapes are difficult tasks, because shapes are often

1

corrupted with noise, occlusion and distortions. Shape descriptors are simply a set of numeric features vectors that are generated to describe a given shape. It should be invariant generally changed even in case of translation, rotation, and scaling caused by viewpoint changes due to camera/object motion [8]. Most of the shape based image retrieval systems extract the information shape based features vectors from the image query and database image, and compute the similarity measure between both images based on the spatial distance functions. The low distance value indicates the closest similarity and specifies the list of images to be extracted based on best matching [9]. Figure 3.1 shows the high-level block diagram of a basic CBIR system.
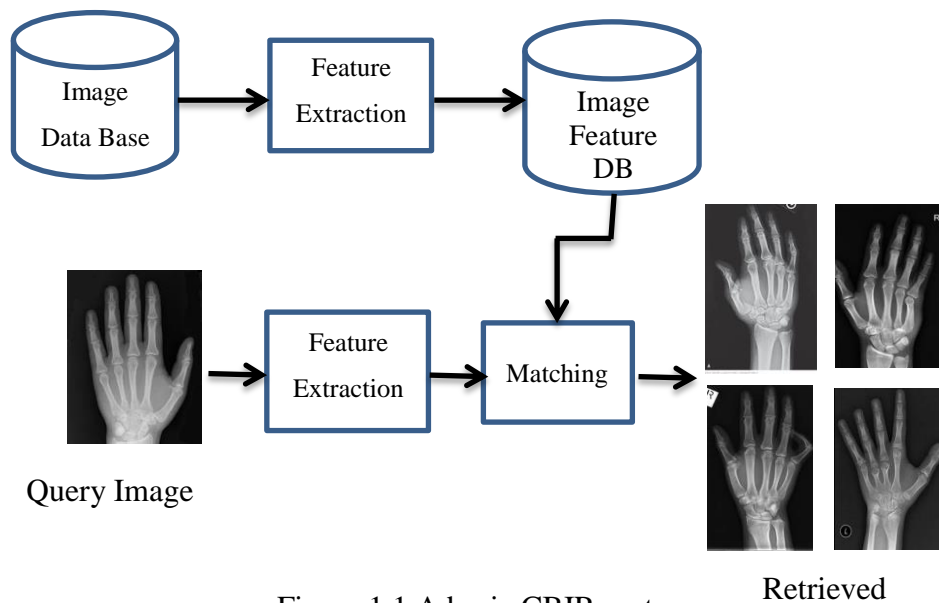
Figure 1.1 A basic CBIR system

1.2 Aim and Objectives

- To obtain images frequently from a huge database dedicated to images based upon the relevance of the object within a set of segment objects; calculate the histogram and statistical texture feature vectors in order to identify the similarity.
- To obtain an images frequently from a huge database dedicated to images upon the contour of an object, and compute CCH, which is used to describe a given shape.
- To improve the original LBP by proposing a novel extension named uniform extended local ternary pattern (UELTP) for CBIR.

2

- To locate mid-sagittal plane in T1-weighted MRI images by using the properties low intensity value of the IF region.
- To detect the rotational angle in the brain slices, by determining the MSP of the brain object.
- To detect the tumor region, by applying K-means clustering and using connected components label.
- To investigate the effects of different types of local texture features on CBIR and to determine MSP in MR brain slice.
- To diagnose melanoma skin cancer, by using texture feature and ABCD rule.

1.3 Thesis Outline

The sections of this thesis comprises of five chapters which are structured as follows:

Chapter Two: This chapter presents the fundamental features extraction techniques for CBIR and medical diagnosis images; and similarity and retrieval measurements.

Chapter Three: This chapter is intended to describe a set of algorithms used in medical images retrieval and diagnosis. Preprocessing image algorithm, Object segmentation algorithms, low-level extraction algorithms, local texture feature algorithms, compute rotation angle of object algorithm and detection of MSP for tilt estimates brain object algorithms.

Chapter Four: This chapter presents the experimental results of the application of the algorithms detailed in chapter three.

Chapter Five: this chapter summarizes the main research achievements, draws conclusions related to image retrieval and pathologies diagnosis of this research; and it also outlines future directions and research work.

Chapter 2: Fundamentals of CBIR and Image Diagnosis

2.1 Features Extraction Techniques

We can define a feature as the capture of specific visual character of an image completely as a whole or regionally through a group of pixels.The extraction of any feature is a way of extracting useful information from images. This section introduces three features: color, texture and shape. In order to achieve a high degree of discrimination for the comparison process, these features should be integrated [10].

2.1.1 Color Features

Color is the one mostly used visual feature in image retrieval. It is relatively strong to background complication and independent of image size and orientations [10]. Most CBIR systems use color space, histogram, moments and color coherence vector to represent color. Color features are one of the most widely used features in low-level features (color, texture, and shape). The performance and efficiency of the color feature are highly dependent on the color space and its quantization [11].

2.1.2 Texture Feature

The image texture is characterized by the reflection of the spatial distribution of the gray contents of the image, in addition to the relationships between pixels pairs of the image and its surrounding. Texture provides a measurement of the regularity, roughness, and smoothness of a certain regions. Textural features extraction approaches consist of two approaches: statistical and structural. In the statistical method, the simplest texture features are used to calculate the first-order statistics, such as mean and variance measurements from the gray intensity values of the image, and the second-order, such as Gray level co-occurrence matrices GLCM, Local Binary Patterns (Ojala et al. [6]) and Local Ternary Pattern (Tan and Triggs [12]).

2.1.2.1 Local Binary Pattern

The original LBP operator describes the texture in the image by dividing the image into cells. In each cell, the intensity values of its neighboring pixels is compared to the gray value of its center pixel and the result is represented as a binary code, which is usually converted into decimal number for convenience [13]. Figure 2.1 illustrates an example of the binary threshold process of the circular $((g,r) = (8, 1))$ neighborhood. The histogram of the resulting image is used for image retrieval.
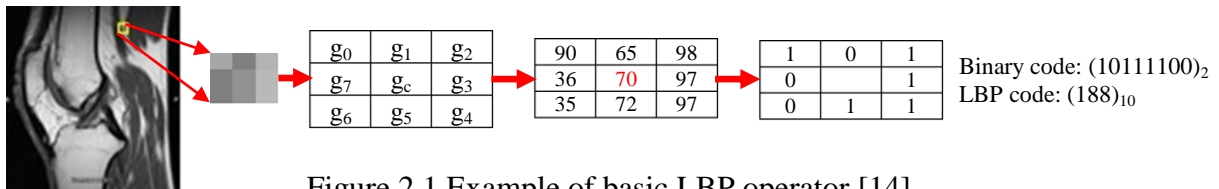
Figure 2.1 Example of basic LBP operator [14]

The existence of features invariable to rotations of the input image is recommended in numerous applications of texture analysis. Ojala et al. [6] extension a new operator called uniform patterns (ULBP). The count of bit wise varying from 0 to 1 or from 1 to 0 in each circular pattern of the LBP code gives the uniformity measure U.

- **Average Local Binary Pattern**

ALBP is an extension to LBP feature in describing local texture structure. This method is based on comparing each neighbor pixel around the center pixel with the computed average value of all neighbor pixels around their center [15].

- **Block Local Binary Pattern**

BLBP features provide the discriminatory power of LBP texture features, and improve the encoding of LBP texture features and classification accuracy. The BLBP features extracts intensity differences between the center pixel and the surrounding average intensity values of pixels in blocks, thus more intensity values of pixels in blocks can be shared, containing different information that is not captured by the original LBP features.

2.1.2.2 Local Ternary Pattern

The LBP is sensitive to noise, because a small gray change of the central pixel may cause drastic changes of the LBP code. In order to address such a flaw, extended the basic LBP to a

version with three-value codes (-1, 0 and 1), that is less sensitive to the noise and more discriminatory in uniform regions called Local Ternary Pattern (LTP). The LTP code is generated by comparing the intensity values of the neighboring pixels with the gray value of its center pixel, threshold (t) used to improved resistance to noise.

2.1.3 Shape Feature

Shape descriptors can be divided into two main categories: region-based and contour-based methods (boundary based). Region-based methods use the whole pixels within a shape region and they are considered to obtain the shape description; compared with the contour based method, it requires a computation cost and more storage. In this thesis, we used chain code for images retrieval and compactness index and dispersion Irregularity for image diagnosis.

2.1.3.1 Chain Code

Chain codes were introduced by Freeman [16] and were used to represent a boundary of the shape of separated objects in the image by registering the list of edge points along a contour and specify contour direction at each edge in the list of numbers. The directions of each edge are quantified into one of the 4-directions or 8-directions. The generated chain code based on determining the starting point at the first edge in the contour list, going clockwise around the contour, traversal from one pixel to the next boundary pixel.

2.1.3.2 Compactness Index

Compactness index is one of the most popular methods used for gauge and quantifying the circularity of the skin lesion. It is based on two parameters: perimeter and area. The compactness is represented the proportion between the area of the object A_s and the area of a circle A_c that can be traced with the same perimeter.   C = As/Ac = (Area of a shape)/(Area of circle) $A_c = \dfrac{P^2}{4\pi}$ Thus $C(S) = \dfrac{4\pi A_s}{P^2}$ Where A_s is the count of pixels of the lesion, and P (circumference) represents the count of edge pixels. The efficiency of the Compactness index is depends on the enclosed boundary of the object shape. For a circular object, the value of C(S)$\simeq$ 1,   which   represent   the   greatest   degree   of   compactness   index   [17].

2.1.3.3 Dispersion Irregularity (IR)

Dispersion IR (irregularity) is another feature suggested by Mark and Alberto [17] to deal with an object that has an irregular shape such as a convoluted shape.

Chapter 3: Principles of Medical Systems Design for Image-Based Diagnosis

3.1 Methods and Tools

In general, the method suggested follows three phases. The first step is pre-processing, by using histogram equalization, linear contrast enhancements, Gaussian filter, median filter and sharpening filter. The second step is image segmentation by applying connected component, K-means clustering and snakes methods. The third step is feature extraction. Figure 3.1 illustrates the method system through a block diagram.
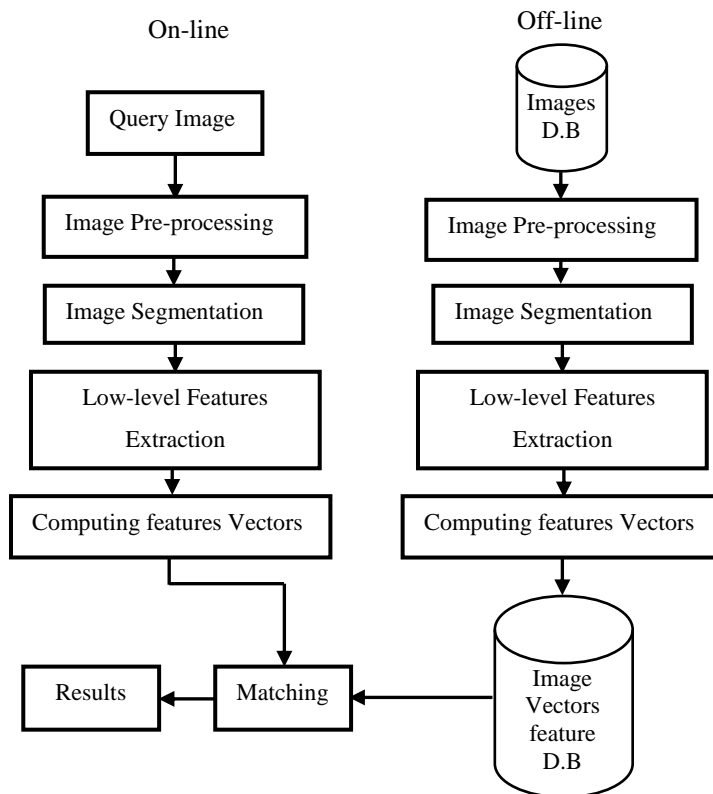
Figure 3.1 Image retrieval system by using low-level feature extraction

3.1.1 Preprocessing

The aim of the preprocessing approach is minimizing the influence of pixels lighting alteration prior to classification. Hence, it is necessary to apply image enhancement before performing any image segmented and texture analysis [18]. The preprocessing proposed in this thesis consists of many filter: histogram equalization, linear contrast enhancements, median filter, sharpening filter and Gaussian filter [19].

3.1.2 Image Segmentation

3.1.2.1 Connected Components

The relation between two or more pixels is defined through pixel connectivity. There are two conditions to accomplish the pixel connectivity, the brightness of pixels and their spatial adjacency. For the formulation of the adjacency measure for connectivity, we firstly employed the representation of the neighbourhood area. Figure 3.2 illustrates part of a binary image, which has two connected components that are based on 4-connectivity. If these two connected components are combined into one, that means, the connectivity is based on 8-neighbors.
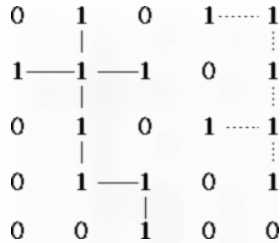
Figure 3.2. Two connected components based on 4-connectivity

For many applications of automated image analysis, it is important to partition the binary image into objects. To extract the connected components, suppose A is a binary image which contains one or more connected components. We create an array X_o which has the same size as the array containing A. The extraction process consists of starting with X_o and finding all the connected pixels, by applying the following iterative procedure [20]:

$$X_k = (X_{k-1} \oplus B) \cap A \quad k = 1,2,3,\dots \tag{3.1}$$

Where A is a test image that contains one or more connected components, B is an appropriate structuring element. The iterative procedure is terminated, when $X_k=X_k-1$ and X_k contain all the connected components of A.

3.1.2.2 K-means Clustering

K-means clustering is one of the most popular algorithms in clustering and segmentation. It is an unsupervised clustering algorithm to segment the input data points by using image features into multiple K classes/groups. The K-means algorithm basically includes the following stages [21]:

- Initialization: which defines the count of clusters K, so-called centroid, and randomly creates the position of the centers for each cluster,

- Assignment of each data point of the data set to the nearest cluster center, by calculating the distance between data set and cluster center by applying Eq. (3.2) and

- Update cluster centroid for the new clusters that were assigned new data points and other clusters that lost data points. Stages 2 and 3 are repeated until there is no significant change of data points between the K clusters, i.e. when the center does not move.

$$F = \sum_{j=1}^{K} \sum_{i=1}^{n} (x_i^{(j)} - c_j)^2 \tag{3.2}$$

Where $x_i^{(j)}$ denotes data point, c_j is the cluster center and n is the count of data point.

The quality of the final clustering results will depend on the selection of the appropriate number of clusters K. In this thesis, the silhouette method [22] is used to analyze the clusters results and to choose the most adequate K cluster.

3.1.2.3 Active Contours Model

Active contours model, also called snakes, which was introduced by Kass et al. [23]. The active contours method is used for the segmentation into two parts (object, or foreground and background) of the 2D grayscale image as shown in Fig. 3.3. This technique requires initial contour as a starting contour for image segmentation. The shape of contour changes and

moves towards the boundaries of the desired object, the moving contour technique is based on the equation usually derived from numerical method and finally, it completely shrinks and wraps around the object [24].
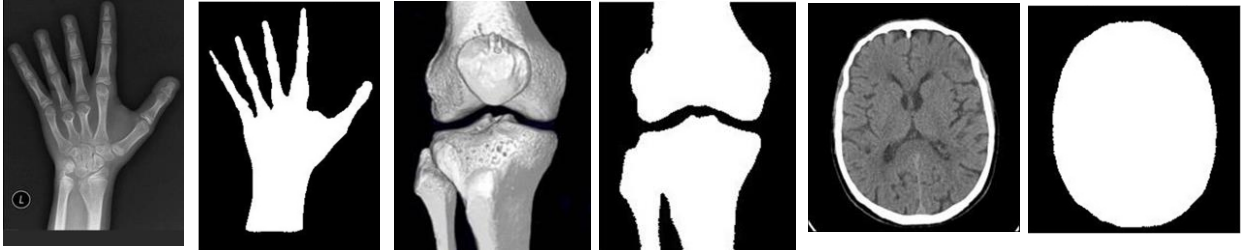
Figure 3.3 Example of 2-D grayscale segment for hand, knee and brain slice images into foreground (white) and background (black) regions by using active contour model [14].

3.1.3 Color Features Extraction

The proposed method for image retrieval is based on the connected components and interest of objects to generate the color histogram feature vectors. These resulted vectors are used to retrieve images from a large image database.

   Algorithm 3.1 to extract the Connected Components Object [2]:

- Input the query image from the user,

- Convert RGB color space into a gray scale by forming a weighted sum of the *R, G*, and *B* components: $0.2989 \times R + 0.5870 \times G + 0.1140 \times B$

- Calculate the threshold of the gray scale image by applying Otsu's method [25],

- Convert the gray scale image into a binary image based on a threshold,

- Enhance the output of the binary image by removing the small objects (e.g. area-size< 50 (pixel)),

- Calculate the connected components of the objects from the binary image by applying equation (3.1),

- Select the maximum connected components object area, and determine their locations.

   The Figure 3.4-(c) through Figure 3.4-(I) show the results obtained by segmenting the binary image into connected components objects, and the area size of each object. Figure 3.4-(d) represents the maximum size of the object.

(a) Query image   (b) Labeled obj. image   (c) Object No=1, Size= 1168   (d) Object No=2, Size= 5228   (e) Object No=3, Size= 371

(f) Object No=4, Size= 3811   (g) Object No=5, Size= 495   (h) Object No=6, Size= 159   (i) Object No=7, Size= 3484
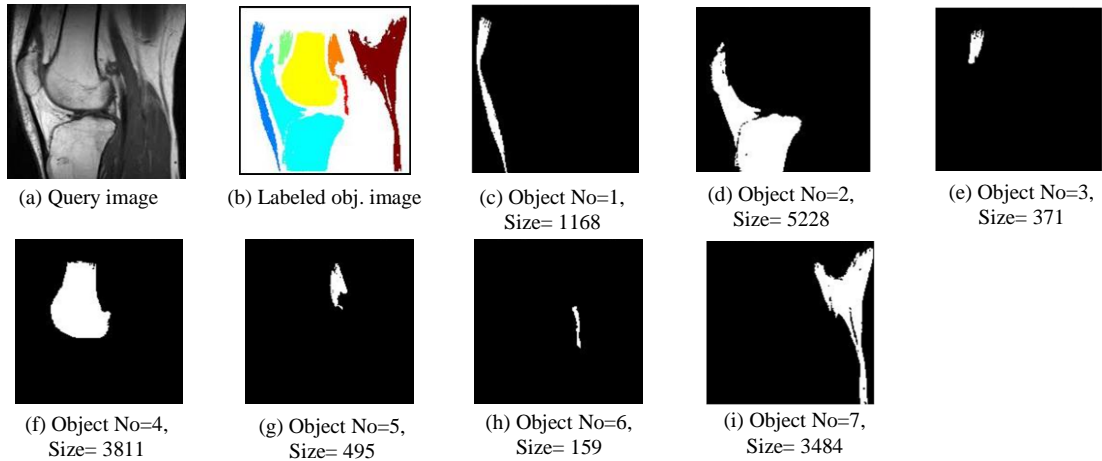
Figure 3.4 (a) Query image, (b) Labeled connected   component image, (c-i) the objects of connected components of query image and area size of each object [2].

3.1.4 Texture Features Extraction

In this thesis the image retrieval by using texture feature consist of two methods:

3.1.4.1 Gray-level Co-occurrence Matrices

Algorithm 3.2 to extract the texture features:

- Input the query image from the user,

- Convert RGB query image into gray scale image,

- The largest object area is automatically selected,

- Compute four GLCM matrices for each direction $(0^{\circ}, 45^{\circ}, 90^{\circ}, 135^{\circ})$,

- For each GLCM matrix compute the statistical features such as Energy, Homogeneity, Contrast and Correlation,

- Compare the results of statistical features between database images and query image by using distance metrics, and retrieve the images based on minimum distance.

3.1.4.2 Extended Local Ternary Patterns (ELTP)

Extended Local ternary Pattern (ELTP), is dislike the mentioned operator due to its independency on unchanged (t). Whereas the local pattern threshold (*t*) is computed automatically based on local features neighboring pixels of the current pixel that are statistically computed [26].

$$ELTP_{p,r} = \begin{cases} 1 & g_p - g_c \geq (\sigma \times \alpha) \\ 0 & |g_p - g_c| < (\sigma \times \alpha) \\ -1 & g_p - g_c \leq -(\sigma \times \alpha) \end{cases}$$

(3.3)

where σ represents the standard deviation of the points that are neighboring the current pixel and α represents the used scaling factor, its value ranged from 0 to 1. The calculate the rotation-invariant. The calculation of the $ELTP_{p,r}$ features $ELTPU_{p,r}^{riu2}$ and $ELTPL_{p,r}^{riu2}$ is done by using the same operations that usually used to transform $LBP_{p,r}$ to $LBP_{p,r}^{riu2}$.

3.1.5 Shape Feature Extraction

In thesis, we focus on contour-base methods to compute the chain code histogram (CCH) and calculate the shape feature vectors for the aim of similarity. There are some disadvantages of the chain code method, which are sensitive to rotation, flipping changes and scaling. In this thesis, to solve the problems of image rotation and flipping, by applying the second-moments method to calculate the rotation angle, analyzing the data of the chain code histogram directions and finally finding the similarity between the horizontally/ vertically flipped shapes and the original shape.

3.1.5.1 Rotation Normalization

A boundary of any regular or irregular object after apply rotation process has different output of chain code. Image moments play a very significant role in object discrimination and shape analysis. The proposed system uses the second-moments method to calculate the angle between the x-axis and the major axis of the ellipse [27]. The shape centroid is represented by the two coordinates (x_c, y_c), the angle θ between the major axes (long line) and the x-axis, and w and l the major and minor axes, respectively, as shown in Figure 3.5.
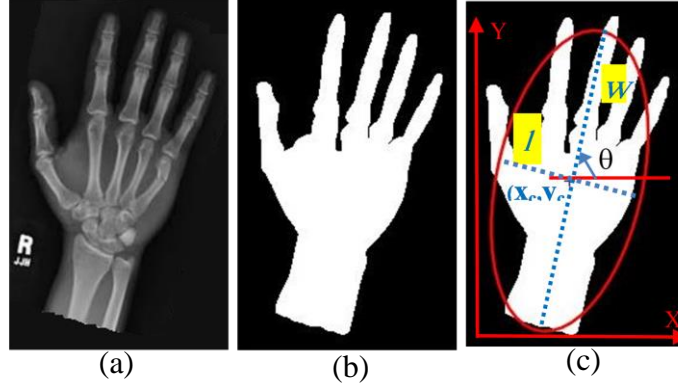
Figure 3.5 Rotation angle of MRI scan hand image, (a) original image, (b) binary image after processing and extracting the connected component object, (c) identification of tilt angle by using analytic geometry of the rotation ellipse, [28].

3.1.5.2 Boundary Extraction

The creating of the chain code is based on extract the boundaries of the shape. Let A is represented binary image with size N × M, the background pixels represented by the value 0 and foreground or shape represented by the value 1.

   Algorithm 3.3 of extracting contour boundaries for the chain code [28]:

- Select object of interest by applying *Algorithm 4.1*,
- Denote the boundary of the selected object(A) by β(A),
- Erode *A* by using structuring element *B*,
- Extract the boundary by applying equation:

$$\beta(A) = A - (A \ominus B)$$

3.1.5.3 Chain Code Histogram

The frequency distributions of the occurrence of the diverse directions reflect the shape of the object. *Algorithm 3.4* of computing the CCH of the object [28]:

- Extract the boundary of the object by applying *algorithm 3.3*,
- Indicate the starting pixel location on the boundary of the object region,
- Save the location of the starting point,
- Test each pixel on the object boundaries in a counter-clockwise direction,
- **For** each pixel located on object boundaries **do**
- Select the boundary directions according to the 8-direction,

- Save the output result in an array or a list,
- **End** For,
- Count the frequencies that correspond in each chain code number, from 0 to 7.

3.1.5.4 Horizontal and vertical flipped shape

A new method is proposed to solve the problem of flipping; this method is based on analysing the CCH data and then finding the similarity between the horizontally/vertically flipped shape and the original shape according to the histogram directions. Table 3.1 illustrates the matching between the CCH directions of the original object image and the flipped object shape (horizontal and vertical).

Table 3.1 Comparison between the CCH directions to identify similarities between the input image and the flipped image [28]

Chain-code 8-directions	Horizontal flipping 8-direction	Vertical flipping 8-direction
0	0	4
1	7	3
2	6	2
3	5	1
4	4	0
5	3	7
6	2	6
7	1	5

where the CCH value of the original object at zero direction is equal to both the CCH value of horizontal flipping at zero-direction and the CCH value of vertical flipping at 4-direction.

Algorithm 3.5 of detecting the flipping of the object [28]:

- Compute the CCH to the query and database images by applying **algorithm 3.4**,
- Save the CCH results into vector1 and vector2 respectively,
- Find horizontal flipping by computing the similarity score between vector1 and vector2 based on the index direction between column 1 and column 2 in Table 3.1,
- Find vertical flipping by computing the similarity score between vector1 and vector2 based on the index direction of column1and column 3 in Table 3.1.

For example, Figure 3.6-(a) shows the object shape and indicates the different 8-directional chain-code boundary numbers. The boundary in Figure 3.6-(b) depicts the horizontally flipped image of the boundary in Figure 3.6-(a) and the boundary in Figure 3.6-(c) depicts the vertically flipped image of the boundary in Fig. 3.6-(a). Table 3.2 illustrates the CCH results of the objects of Fig. 3.6 when applying the proposed Table 3.1, the CCH values of the original object (for example) at 2-direction is 4, and it matches both flipping: horizontal flipping at 6-direction, and vertical flipping at 2-direction.
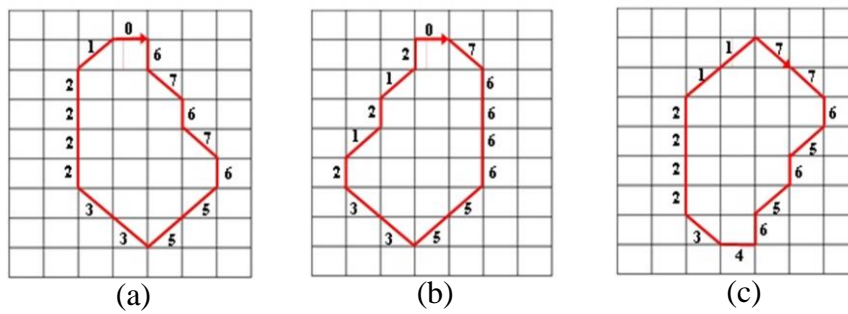
Figure 3.6. Example of the flipping method; (a) contour of the shape indicating the 8-directional of the chain code; (b) horizontal flipping; (c) vertical flipping

Table 3.2. Results of the 8-direction CCH to the original and flipped images in Fig. 3.6 [28]

8-directions of chain code	CCH Original object	CCH Horizontal flipping	CCH Vertical flipping
0	1	1	0
1	1	2	2
2	4	3	4
3	2	2	1
4	0	0	1
5	2	2	2
6	3	4	3
7	2	1	2
Total contour	15	15	15

3.2 Applying Feature Extraction Techniques for Brain Tumor Diagnosis

3.2.1 Color Feature Extraction for Brain Tumor Diagnosis

Intensity Color Feature is a powerful method used to diagnose the pathologies. The brain is one of the largest and most complex organs of the human body. Healthy human brain tissues are present in an approximate bilateral symmetry, while the growth of tumors causes asymmetry in the affected parts of the brain. The proposed method calculates asymmetry based on the intensity difference between the two sides of a mid-sagittal plane (MSP).

3.2.1.1 Mid-Sagittal Plane (MSP)

The MSP is an important feature used for detecting bilateral asymmetry of the brain slice such as bloc effects and unbalanced tissues density due to a tumor growth or bleeding, etc. The inter-hemispheric fissure (IF), which is the longitudinal dark and deep groove located in the midline boundary between the two cerebral hemispheres, is called MSP as shown in Figure 3.7-(a). The IF contains cerebral spinal fluid (CSF). This leads to the intensity differences between the IF and the enclosure tissue gives a weak MR signal on MSP [29] as shown in Figure 3.7-(b).

(a)   (b)
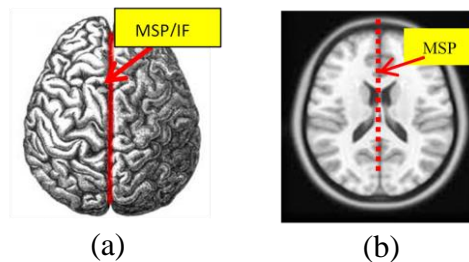
Figure 3.7. The human brain; (a) medial inter-hemispheric fissure visible in red line, (b) T1-Weighted MRI brain axial slice with indicating the MSP by red dotted line

3.2.2 Brain Tumor Detection

The proposed method consists of two sections: first, detecting a tumor slice, by using bilateral symmetry to distinguish a slice that contains tumor area, and second, detecting a tumor region, by applying K-means clustering followed by connected component labeling. The Figure 3.8 illustrates the method system through a block diagram.
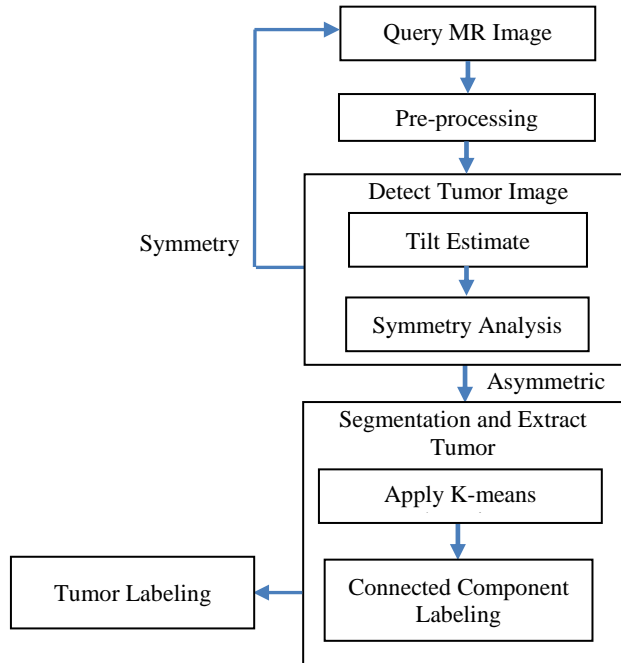
Figure 3.8. Block diagram of the brain tumor detection [30]

3.2.2.1 Preprocessing of Brain Slice

Image preprocessing is a significant step in medical image diagnosis. The preprocessing method is depend on the results of convert the RGB input image into gray scale image, removing the noise, and enhancing the image.

3.2.2.2 Tilt Estimate

The symmetry axis on each brain slice depicted a center line for detecting bilateral asymmetries such as tumor effects and lopsided tissues [31][5]. The proposed system uses a method to detect the rotational angle in the brain slices, by determining the MSP of the brain object. The proposed system is based upon the properties of low intensity value of the IF region as shown in Fig. 3.9.

Algorithm 3.6 of detected MSP for tilt estimates of the brain object slice **[30]**:

- Convert RGB image to gray scale and binary images,
- Fill the holes of the binary image by using an algorithm based on morphological reconstruction,
- Compute the centroid of the brain slice object,

17

- Generate a straight line that passes through the centroid and rotates from $0°$ to $180°$ by $1°$ degree increment,
- **For** each rotate angle θ_o **do**
- Compute the line intensity score by adding the intensity binary values (one's) along the line and keeping a track of the angle.
- End For
- Sort the lines intensity scores with angles θ_o in ascending order,
- Choose a set of lines scores with equal intensity values and maximum repetition,
- Choose the angle θ_o and intensity score that represents the middle value among a set of equal intensity lines,
- On the gray scale image, compute line intensity L_1 at angle θ_o,
- On the gray scale image, perform a two shifting process around θ_o, between -1 to -10 and 1 to 10 and compute the intensity score of these shifting L_2 and L_3 respectively,
- Compute the best-fit line by taking the lower intensity score between L_1, L_2, and L_3.

| (a) | (b) | (c) | (d) | (e) |
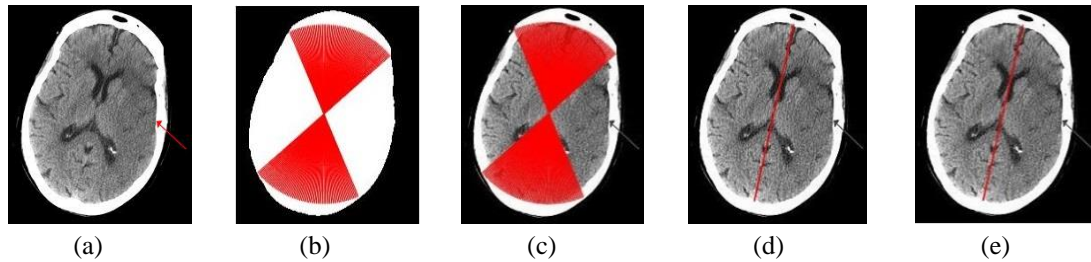
Figure 3.9. Extracted mid-sagittal plane from brain axial slice of type T1-Weighted MRI; (a) original image; (b) binary image with filling holes, indicating the set of equal intensity longer lines by red lines; (c) gray scale image indicating the set of longer intensity lines; (d) selected mid line from set lines; (e) improved the position of the midline by applying left and right shifting [30]

3.2.2.3 Bilateral Symmetry Analysis

The healthy brains display usually bilateral symmetry, i.e. the regions between the MSP are similar in shape and relative location, while areas affected by tumor or pathology are not symmetrical [32]. In this thesis, the Bilateral Symmetry can be calculated by dividing the area of axial, or coronal slices of objects into two sides according to the MSP, then the intensity value between two sides are calculated as shown in Figure 3.10.

| (a) | (b) | (c) | (d) |
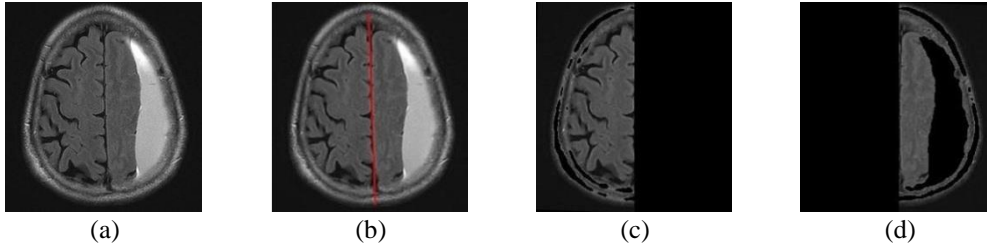
Figure 3.10. MRI brain slice image. (a) brain hemorrhage, (b) brain MRI axial slice indicating the MSP by red line, (c) and (d) asymmetry between two sides of brain image

3.2.2.4 Segmentation and Extract Tumor

Algorithm 3.7 for K-means clustering segmentation and extracting the tumor **[30]**:

- Convert RGB image into gray scale,
- Input the initial no of cluster value as 6,
- Compute the K-means clustering by applying the steps in section 3.1.2.2 [21],
- Analyse the cluster results and candidates for the useful K cluster by applying the Silhouette method [22],
- Separate brain objects from the image background by performing the connected components approach by applying equation (3.1),
- Perform connected components label to detect tumor location.

3.2.3 Local Texture Feature Extraction for brain Tumor Diagnosis

In this thesis, the MSP extraction is based on computing the local texture feature between IF and the surrounding tissue, by applying LBP techniques [7]. All the processes of detecting MSP are shown in Figure 3.11.
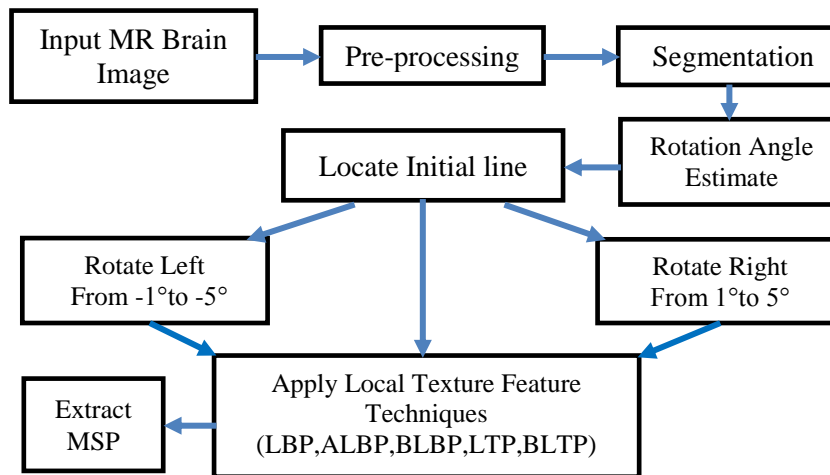
Figure 3.11. Block diagram of extract MSP [7]

3.2.3.1 Rotation Angle Estimate

In some cases, the patient's head may be tilted during the scanning process. MSP is the plane that travels vertically and divides the brain into similar hemispheres. MSP is employed to correct rotation and tilting of the brain slice [33]. The proposed method is based on the second-order area moments method to detect the brain tilted angle, by calculating the angle between the x-axis and the major axis of the brain ellipse. The rotation angle resulted is used to determine the initial line of the MSP [27].

3.2.3.2 Block Local Ternary Pattern

Algorithm 3.8 for calculating the Block-LTP code [7]:

- Input the training image from the image set,
- Initialize the values of radius r_1 *and* r_2,
- Convert RGB color space image into a gray scale,
- **For** each center pixel t_{c1} at radius r_1 **do**
- **For** each neighbor pixel t_{g1} around the t_{c1} **do**
- Calculate the average value to the all neighboring pixels t_{g2} around the center pixel t_{c2} at radius r_2,
- Create a new window with size (t_{g1}, r_1),
- Compute the LTP code number,
- Split the LTP code result into two different parts; positive (high) and negative (low),
- End For
- End For
- Calculate the summation of each part of LTP code separately.

3.2.3.3 Detecting Mid-sagittal Plane

The proposed **algorithm 3.9** for detecting the MSP line is implemented in the following steps [7]:

- Convert RGB image into gray scale and binary images applying Otsu's method [25],

- Calculate the connected components of the objects of the binary image by applying equation (3.1) and selecting the maximum connected components object area,

- Generate an initial line according to:

    1. Calculation of the centroid of the segment object image,

    2. Calculation of the length values of major-axis,

    3. Calculation of the angle of a rotating object ϕ,

- Rotate the initial line from 1° to 5° and -1° to -5° by 1° degree increment,

- **For** each rotate angle **do**

- Compute the LBP techniques and Block-LTP by applying **algorithm 3.8** with keeping a track of the angle,

- **End** For

- Estimate the best-fit line by taking the minimum of sum results among the values of Low-LTP and Low-BLTP; and High of sum results among the values of High-LTP and High-BLTP.

3.3 ABCD Rule Features Extraction and used in for Melanoma Skin Cancer Diagnosis

Skin cancer is a dangerous health problem. It is caused by the development of abnormal cells that have the ability to spread rapidly to all organs of the human body through the lymphatic system or blood [34]. Melanomas are the most aggressive yet harmless kind of skin cancers.

In this thesis, we used the automatic method to diagnose melanoma skin cancer. This approach evolves in three sequential steps. First, the lesion image is preprocessed using low-pass filters, linear contrast adjustment, and histogram equalization. Second, the lesion is segmented using connected components objects method. Third, the ABCD rule (Asymmetry, Border, Color, and Diameter) and statistical texture features are computed from the lesion. The ABCD rule is used to calculate the TDV score, whereas the texture analysis uses methods such as Gray Level Co-occurrence Matrix (GLCM), and four statistical measures are extracted: energy, entropy, contrast and correlation [35].

3.3.1 Rule Features

3.3.1.1 A: Asymmetry

Asymmetry is an important feature used for realization of the symmetry of the object shape, which is very useful in pattern analysis. If the normal mole area is divided into two sides depend on the major and minor axes, the mole border of one side would similar to the other side perfectly. In an asymmetrical mole, the two edges sides do not similar in size or shape, as shown in Figure 3.12. In the example of Figure 3.12, the score of asymmetry is 2.

(a)	(b)	(c)	(d)	(e)	(f)
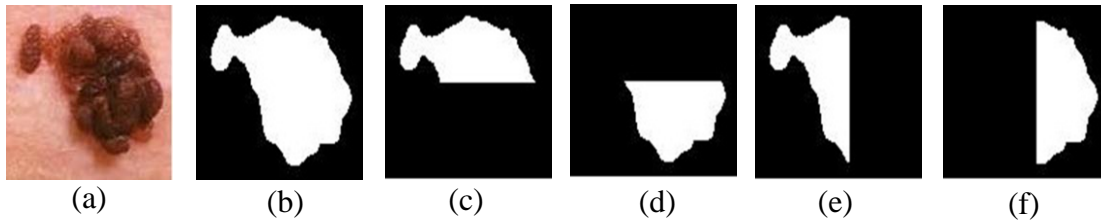
Figure 3.12. (a) Skin lesion image, (b) the result of pre-process and segmented, (c, d, e and f) divisions of the lesion depend on two axes [35]

3.3.1.2 B: Boundary Irregularity

The irregularity of the boundary is an indicator of the growth and spread of the cancerous cell. For an evaluation, in this thesis, the segment lesion is bisected into two sections, and then the Euclidean distance between the centre of the lesion and all pixel boundaries of each section separately is calculated. Finally, the summation of the difference between two lesion parts calculated, as shown in Figure 3.13.

(a) (b)
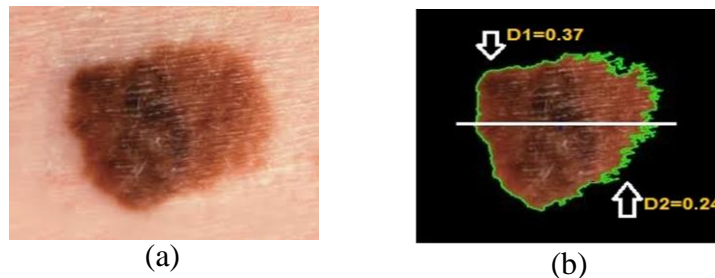
Figure 3.13. (a) Skin lesion image; (b) the two sections of the lesion according to the major axis divisions and the two distances values (D1 and D2) [35]

3.3.1.3 C: Color Index

One early indicator of melanoma is the development more than one color in area lesion colors. Because melanoma cells grow in pigment, they are often colorful around brown or black areas, depending upon the production of the melanin pigment at different depths in the skin [36]. Color index is determined by converting the original color image to the HSV color space and then calculating the distance between each pixel value in the lesion and the color we want to detect. The Eq. (3.4) is used to calculate the difference of colors.

$$\Delta E = \sqrt{(h_1 - h_2)^2 + (s_1 - s_2)^2 + (v_1 - v_2)^2}$$ (3.4)

Where h_1, s_1 and v_1 are represent the HSV color space of the required color and h_2, s_2 and v_2 those of each pixel of the image. The Figure 3.12 shows the result C=4 (red, light brown, dark brown and dark red).

3.3.1.4 D: Diameter

Some moles remain with certain size and never change, but others can grow or change their size. Where the measures of a normal size is less than or equal six millimeters. Bigger moles can indicate signs of trouble.

3.3.1 Using Rule Features in the Classification of Skin Lesions

The Stolz algorithm is used for moles image classification based on calculate the TDV score, to calculate the TDV score is depending on the Multivariate analysis of the four feature and assign them a numeric score: Asymmetry index is (0-2), Border index is (0-8), Colour index is (1-6), and Diameter index is (1-5), and then each of the feature index is scaled by a given weight factor, finally the sum of these weighted scores is used to generate (TDV) [37].

$$TDV = 1.3 \times A + 0.1 \times B + 0.5 \times C + 0.5 \times D$$ (4.26)

This result is used to diagnose benign, suspicious or melanoma skin lesion as follows:

$$Diagnosis = \begin{cases} Benign & TDV < 4.75 \\ Suspicious & 4.8 < TDV < 5.45 \\ Melanoma & TDV > 5.45 \end{cases}$$ (4.27)

23

Chapter 4: Experiments and Results

In this thesis, all stages of the image retrieval and medical diagnosis algorithms are implemented in MATLAB R2016A using a database that consists of 500 images, which contains four different categories: knees, brains, leaves, and hand. Brain images class are taken from the database in [38]. The experimental results of the algorithms used in this thesis are presented in the following sections.

4.1 Applying Color Histogram and Statistical Texture Feature Algorithms for CBIR

We focus on automatic selection of regions of interest connected component object and calculating the color histogram object feature and texture feature retrieval vectors to identify similarity. There are five different categories, which include knees, brains, dinosaurs, hands, and flowers. The system is executed with eight images from each of the five categories and the similarity score is calculated to color and texture for each image. The list of results is displayed as number of objects, maximum size of an object, and co-occurrence statistics measures, as shown in Fig. 4.1.
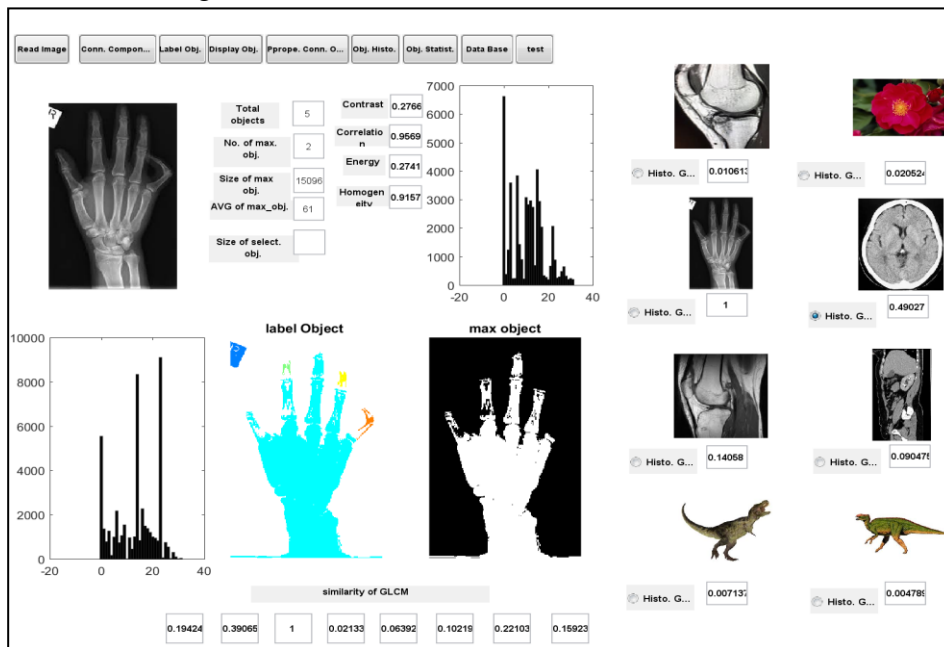
Figure 4.1. User interface of the results of color based and texture similarity between brain and different brains images

The results of average precision and average recall parameters are calculated by using objects histogram and texture based for different category of images are shown in Table 4.1.

Table 4.1. Color and texture (GLCM) based precision and recall analysis

Category	Color (Histogram)		Texture (GLCM)	
	Precision	*Recall*	*Precision*	*Recall*
Knee	0.69	0.20	0.85	0.1
Brain	0.75	0.13	0.60	0.03
Hand	0.79	0.11	0.57	0.03
Flowers	0.88	0.28	0.78	0.24
Dinosaur	0.89	0.13	0.93	0.11
Average	0.80	0.17	0.75	0.10

4.2 Applying Uniform Extended Local Ternary Pattern Algorithm for CBIR

In this thesis, we focus on automatic identification of the object of interest and computing the local texture features vectors for comparison purposes. The regions of interest are roughly identified by applying snakes segmentation method to produce independent objects in an image, segmenting the image into foreground (object), and background regions and then extracting the local texture features (LBP, LTP and ELTP) in each object.

The experimental results of the proposed retrieval system performance are shown based on average precision parameter and recall parameters are calculated., Table 4.2 shows results related to the proposed system based on segmentation objects for various image categories. While, Table 4.3 illustrates the proposed retrieval system performance by using different dimensionality of radius r. In this experiment, the comparison between the proposed methods ULBP and UELTP are given in Table 4.2. It is demonstrated that the $ULBP^{riu2}$ and $UELTP^{riu2}$ reach an average of precision with higher performance than classical LBP and LTP. The precision is 13% and 18% higher for the improved methods, $ULBP^{riu2}$ and $UELTP^{riu2}$, compared to the original versions. The proposed GUI of the system is depict in Figure 4.2.

Table 4.2. ULBP and UELTP based precision and recall analysis based on segmentation object

Category	$ULBP_{8,1}^{riu2}$		$UELTP_{8,1}^{riu2}$	
	Precision	*Recall*	*Precision*	*Recall*
Knee	0.80	0.24	0.91	0.18
Brain slice	0.75	0.28	0.88	0.21
Hand	0.79	0.24	0.83	0.25
Average	0.78	0.25	0.87	0.21

Table 4.3. ULBP and UELTP based precision analysis based on different dimensionality

Category	$ULBP_{p,r}^{riu2}$			$UELTP_{p,r}^{riu2}$		
	(p,r)			*(p,r)*		
	(8,1)	(8,2)	(8,3)	(8,1)	(8,2)	(8,3)
Knee	0.80	0.79	0.77	0.91	0.88	0.90
Brain slice	0.75	0.75	0.73	0.88	0.85	0.86
Hand	0.79	0.77	0.73	0.83	0.83	0.80
Average	0.78	0.77	0.74	0.87	0.85	0.85
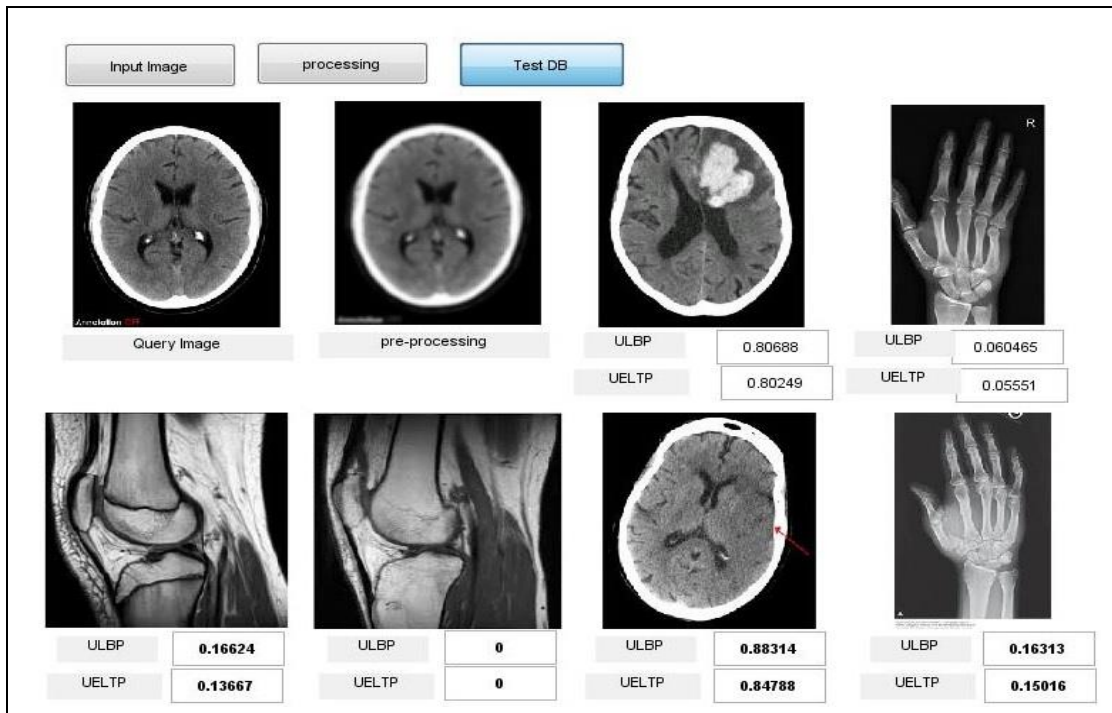
Figure 4.2. User interface of the results of ULBP and UELTP to find the similarity between brain and hand, knee and brain images

26

4.3 Applying Shape Based Algorithm for CBIR

In this research, we used the contour-base methods to compute the chain code histogram (CCH) and calculate the shape feature vectors for the aim of similarity, describing a given shape. For testing the horizontal and vertical flipping, the CCH values to all three different images in Figs. 4.3-(c) and 4.3-(e) are calculated by using the algorithm (3.4). Finally algorithm (3.5) is applied to find the similarity index. The experimental results show that the values of similarity index between query image and flipped image fall within the values greater than 0.90, as shown in Figure 4.4.

| (a) | (b) | (c) | (d) | (e) |
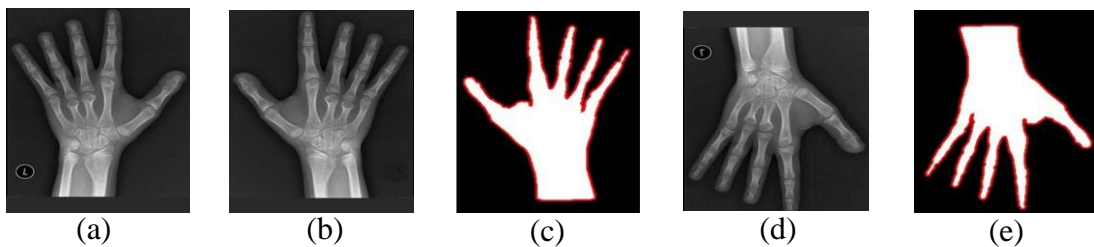
Figure 4.3. Flipped image: (a) original image; (b) horizontally flipped image; (c) contour boundary to the horizontally flipped image; (d) vertically flipped image; (f) contour boundary of the vertically flipped image
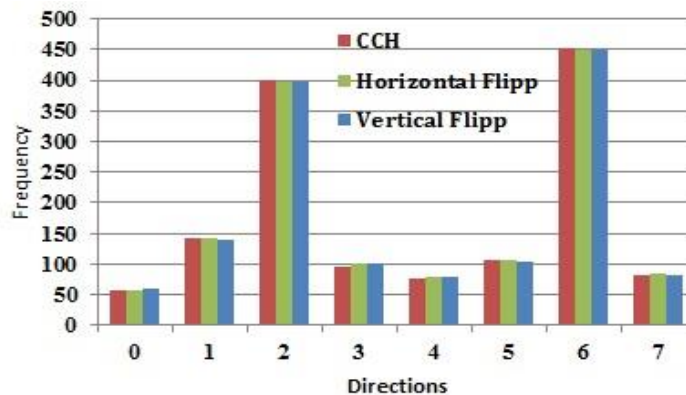
Figure 4.4. CCH of the query and flipped (horizontal and vertical) images

The system executes six images from each of the four categories and calculates the similarity to both CCH and CCH-flipping between query image and database image. For each image, the system can display some results of the images that describe the enhancement of the query image, boundary object image, and chain code histogram objects for both the query image and the database images, as shown in Figures 4.5.
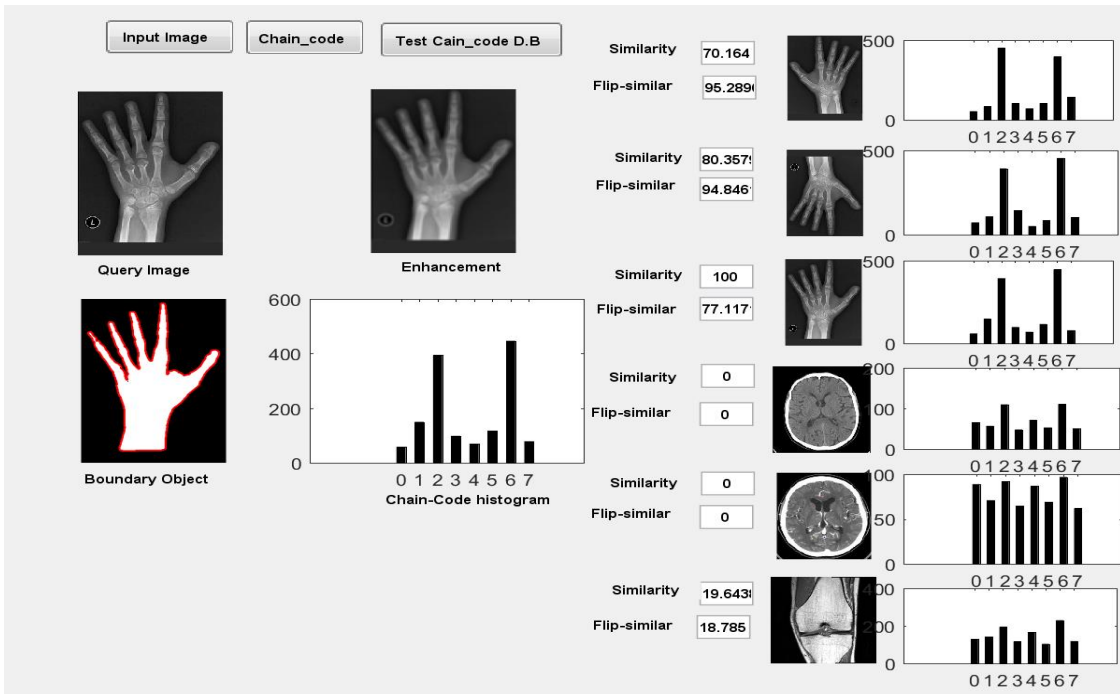
Figure 4.5 User interface of the results of CCH and flipped-CCH similarity between hand image and different images

To evaluate the work of the proposed system, the precision and recall parameters are calculated by computing the histogram to both chain code and flipped image; four different categories of medical images are shown in Table 4.4.

Table 4.4. CCH and CCH with flipping based precision and recall analysis

Category	CCH		CCH with flipping	
	Precision	*Recall*	*Precision*	*Recall*
Brain	0.62	0.23	0.64	0.19
Hand	0.83	0.22	0.89	0.23
Leaves	0.71	0.20	0.70	0.22
Knee	0.65	0.18	0.67	0.20
Average	0.70	0.21	0.73	0.21

4.4 Applying Local Texture Features Algorithms for Locating MSP in Brain Slice Image

We compute the local texture features between the initial MSP and neighboring pixels of the brain tissue by applying algorithm 3.8 and algorithm 3.9. The proposed system consists of four stages: preprocessing, segmentation, Tilt Estimate and applying LBP techniques. For testing the algorithm of MSP detection, Figure 4.6 illustrates an example to detect MSP line. To improve the accuracy of MSP detection, we tested the neighboring area around the initial line, by applying a number of rotation angles e.g. from 1°to 4° by 1° degree increment i.e. clockwise direction as shown in Figure 4.6-e through Figure 4.6-h. Figure 4.6-i through Figure 4.6-l represent the rotation angles e.g. from -1°to -4° i.e. anticlockwise directions around the center.
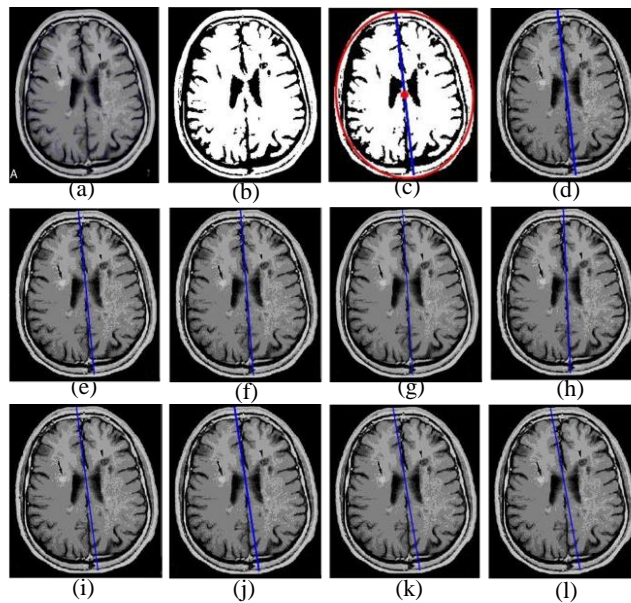
Figure 4.6. Example of MSP detection: (a) original brain slices image; (b) pre-processing and segmentation image; (c) detection of the tilt angle of the brain object; (d) the initial line on gray scale image; (e-h) rotation of the initial line from 1° to 4°; (i-l) rotation of the initial line from -1° to -4°

29

4.5 Applying the Asymmetry and K-Means Clustering Algorithms for Brain Tumor Detection

The proposed system consists of two stages: first, the detection of tumor slices, by testing the tilt process and bilateral symmetry that classify the image into two types, tumor and normal brain images, For testing the MSP's detecting algorithm, Fig. 4.7-a shows image brain slice containing tumor, Fig. 4.7-d shows the process of locating the rotation angle by using middle intensity value. The maximum number of the repetitions for a line with intensity score value of 192, is 84 times, as indicated in Fig. 4.7-d, consequently the rotation angle of middle intensity lines (84/2=42) is 89°. The image shown in Fig. 4.7-e, represents the result of the MSP by red a line. Second, detection of the tumor region, by applying K-means clustering and using connected components label to detect tumor location. Based on the result of cluster K followed by connected component label the tumor is extracted as shown in Fig. 4.7-l.
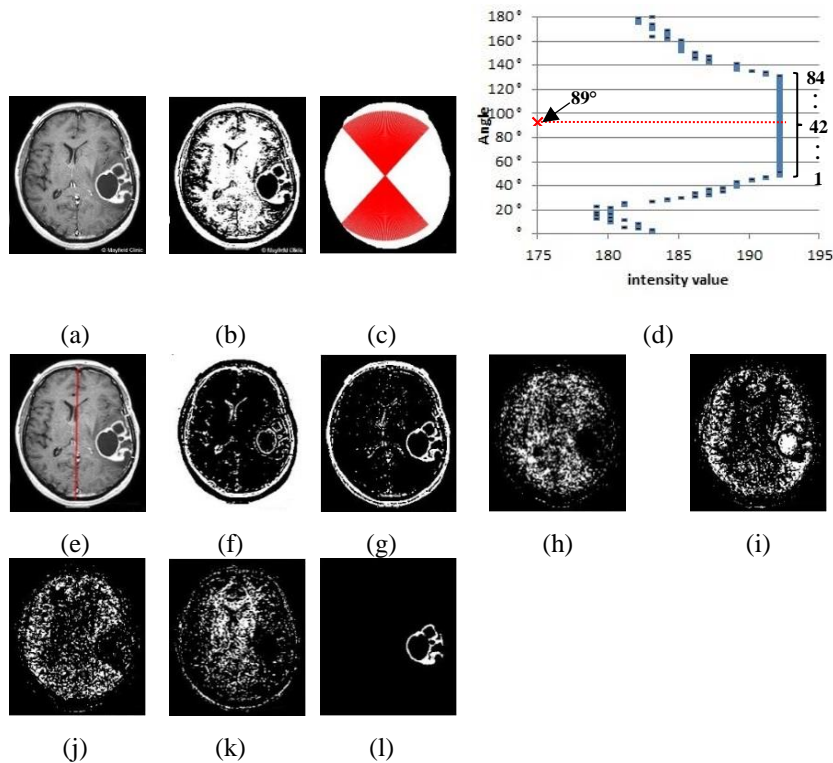
Figure 4.7. The outputs of the extracted mid-sagittal plane, K-means clustering, and detected tumor lesion, (a) Original axial slice image scan, (b) thresholding, (c) Binary image with filling holes, with indicated the set of equal intensity longer lines by red lines, (d) rotation angles from 0°to 180° by 1° degree increment (e) detected MSP (f-k) K-Means clustering results from K=1 to K=6 clusters, (l) Labeling of the detected tumor.

4.6 Applying local texture features to Performance Analysis of K-Means Clustering algorithm for Brain Tumor Detection

In this study, we have proposed segmentation of the brain MRI image using K-means clustering algorithm to generate list of cluster images. The automatic selection of the appropriate cluster image used to detect brain tumor is based on local texture feature and bilateral symmetry, which are computed between the two brain sides.

The proposed method consists of two stages: first, generating a list of cluster images, with the regions of interest objects by applying K-means clustering algorithm. In the second step, the automatic selection of the appropriate cluster image is computed, based on ULBP and brain asymmetry. Figure 4.8 illustrates an example to detect brain tumor.
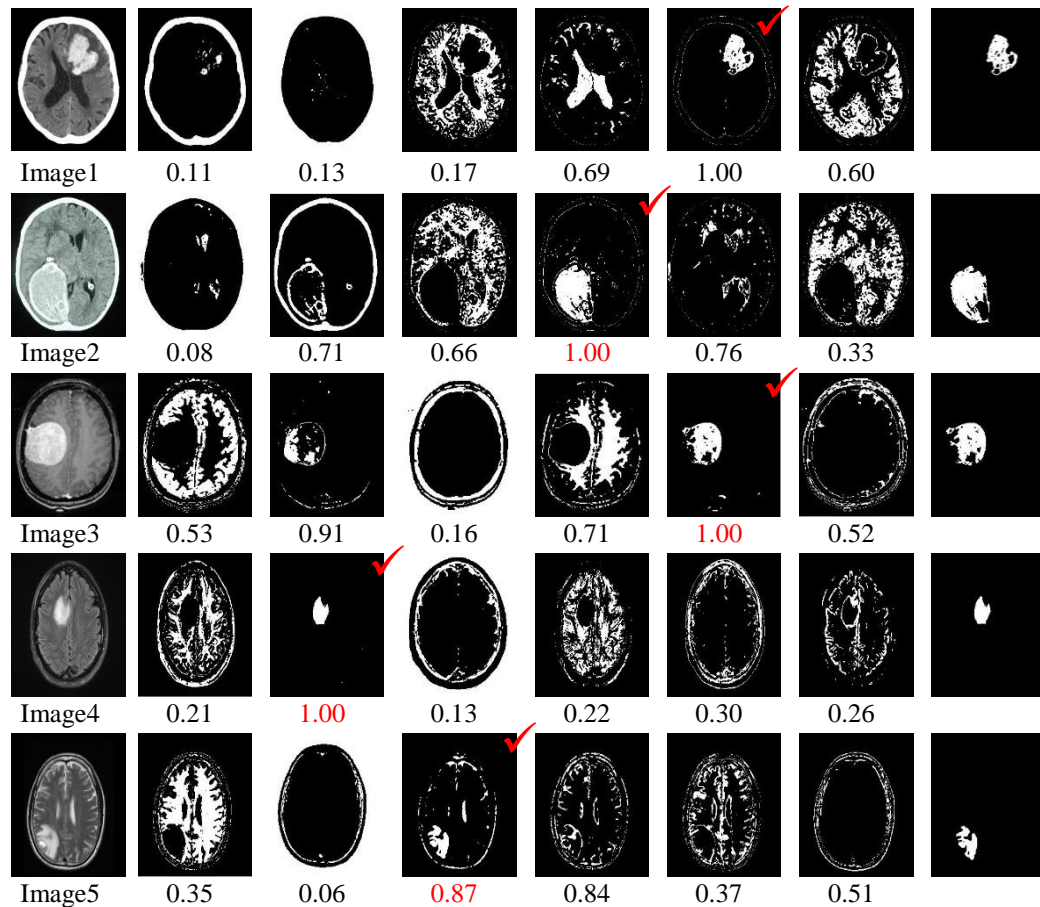
Figure 4.8 Examples of detected tumor lesion from T1-Weighted MRI brain axial slice: first column original images; columns from 2 to 7 results of the K-Means clustering from K_1 to K_6 clusters, with the results of asymmetry values indicated with each cluster image; last column labeling of the detected tumor

4.7 Applying Statistic Texture Feature and ABCD Rule for Diagnosis Melanoma Skin Cancer

In this work, all stages are implemented in MATLAB R2016A with a set of 50 skin lesion images, which contains melanoma and benign skin images. Figure 4.9-(a) depicts the skin lesion image; the segmentation and extraction of the connected components lesion object as shown in Figure 4.9-(b) algorithm have been applied on the grayscale intensity image. The desired segmented image is illustrated in Figure 4.9-(c). For each image, the segmented lesion is surrounded by a solid blue line, and is determined by the centre of mass as shown in Figure 4.9-(d). The final segment is used to calculate the ABCD feature extraction values and statistics features.

(a)   (b)

(c)   (d)
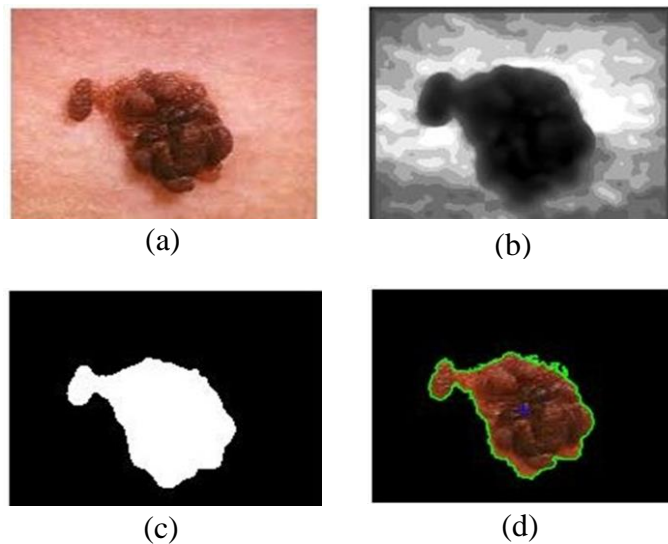
Figure 4.9. (a) Skin lesion image; (b) gray image; (c) segmented image after using connected component method; (d) boundary tracing image and center of mass

Conclusion and Suggestions for Future Work

The major algorithms applied in this thesis are presented in chapters 3 and the results of the proposed works are shown in chapter 4. We summarized the following main findings and contributions of this research work:

- In section 4.1, we discuss the low-level features of color and texture extraction for CBIR. Experiments showed that the proposed method is capable of extracting interesting objects from uninteresting objects and a complex background image without any previous knowledge. The extracted maximum object is expected to be effectively used in object-based image retrieval because it represents the main part of the image. The proposed system has achieved the highest average precision, which is 78%.

- In section 4.2, we discuss the present study presents the Uniform Extended LTP (UELTP) method for the CBIR system. Many conclusions can be extracted; First conclusion, texture features histogram is a good method to retrieval of the matching images from the database. Another conclusion, the experimental results show that the $UELTP_{8,1}^{riu2}$ achieves an average of precision higher in performance than classical LBP and LTP. The experiments show that the performance of $UELTP_{8,1}^{riu2}$ by using segmentation method is powerful for increasing retrieval precision as shown in Table 4.2 and Table 4.3.

- In section 4.3, we discuss the obtained of the matching images from the database based on shape representation by using CCH features. The first conclusion is that chain code histogram is a good method to recognize both regular and irregular objects, as well as independent with regarding to the starting point of the chain code. Another conclusion is that the experiments showed that the proposed method is powerful in increasing retrieval accuracy as shown in Table 4.4. The proposed system has achieved the highest average precision, which is 73%.

- In section 4.4 we discuss the local texture features techniques applied on T1-Weighted MRI brain axial slice images to achieve automatic detection of MSP. New variants of

LTP features, high BLTP and low BLTP, are proposed. There are two conclusions. The first conclusion is that the MSP detection accuracy increases when the intensity of the differences between the IF and surrounding tissue is high. The second conclusion is that there are some cases of brain slice with tumors. The MSP was detected accurately in slices that have smaller tumors. The comparison among the performances of LBP, ALBP, BLBP, LTP, and BLTP, shows that the best result is achieved by using the BLTP method which reaches the best overall performance.

- In section 4.5, we discuss the detection of brain pathologies, such as tumor and brain haemorrhage based on two sections, bilateral symmetry and K-means clustering followed by connected component labeling. The MRI image segmentation is used to detect tumor location using K - means clustering algorithm. Silhouette analysis is a useful gauge to evaluate a candidate K for clustering. The proposed system provides the best results when the connected component labeling process is applied too. The proposed system has achieved the highest average precision which is 94%.

- In section 4.6 we discuss the detection of melanoma based on three phases, ABCD rule of dermatoscopy, statistical texture analysis, and lesion symptoms. The first conclusion is that boundary irregularity is a good indicator to determine the melanoma. Another conclusion is that there are some cases of melanoma where the calculation of the asymmetry index of two different contents sections has not been large, because this method is based on the area (total pixel count of a lesion). The experiments showed that the contrast and entropy are powerful measurements in the characterization of the chaotic and variance of the cancerous skin images. The accuracy of the development system is 90%.

As a suggestion for Future work, by applying machine learning algorithms to improve the overall performance of the proposed systems and used for the detection the MSP and brain tumors, hence that make the system more intelligent.

Contributions of this Thesis

- A new algorithm for detecting the rotational angle in the brain slices is proposed. The main idea of the proposed algorithm is based on low intensity of inter-hemispheric fissure (IF) region and on the estimation of the best-fit line determined by taking the minimum intensity score between a multi shift process lines. The performance of the proposed algorithm in compared with the other work algorithms, which clearly shows the efficiency of the proposed algorithm in terms of accuracy and computationally cost. The results have been illustrated in my published paper [30].

- A new method is proposed to locate MSP in T1-weighted MRI images, based on the computation of the different local texture between inter-hemispheric fissure (IF) region and the surrounding tissue. We proposed a new method by using Block Local Ternary Patterns. The advantage of this method is used to increase the discriminatory power of LBP texture features thus improving the encoding of the texture feature and improving the classification accuracy. The results have been presented in my published paper [7].

- Melanoma skin cancer diagnosis based on the combination of ABCD rule of dermatoscopy, statistical texture analysis, and lesion symptoms is proposed to upgrade the acceptable performance rates of the diagnosis system. The results have been described in my published paper [35].

- A new method for CBIR is proposed. This method is based on local texture feature techniques. The performance of Local Binary Pattern descriptor, Local Ternary pattern and Extended Local Ternary Pattern are evaluated for CBIR. According to the results, uniform extended local ternary pattern more accurate than other descriptors in terms of image retrieval. The results have been explained in my published paper [14].

- A new Image retrieval method based on the connected components and interesting of objects is proposed to generate the histogram and statistical texture feature vectors. These resulted vectors are used to retrieve images from a large image database. It is obvious that the experimental data clearly show the efficiency of the proposed method in comparison to the traditional ROI technique in terms of computational cost. The results have been illustrated in my published paper [2].

- A new method is proposed to performance analysis of K-Means clustering for brain tumor detection. The automatic selection of the appropriate cluster image used to detect brain tumor is based on uniform local texture feature and bilateral symmetry, which are computed between the left and the right half of each clustering image.. The results have been illustrated in my published paper [39].

Selected Bibliography

[1] S. Madhu, "Content based Image Retrieval: A Quantitative Comparison between Query by Color and Query by Texture," *Journal of Industrial and Intelligent Information,* vol. 2, no. 2, pp. 108-112, Nov. 2014.

[2] F. Baji and M. Mocanu , "Connected components objects feature for CBIR," in *2017 18th International Carpathian Control Conference (ICCC)* , Sinaia, Romania, 28-31 May 2017 DOI: 10.1109/CarpathianCC.2017.7970460.

[3] R. K. Lingadalli, and N. Ramesh, "Content Based Image Retrieval using Color, Shape and Texture," *International Advanced Research Journal in Science, Engineering and Technolog,* vol. 2, no. 6, pp. 40-45, Jun. 2015.

[4] E. R. Vimina, and K. P. Jacob,, "Content Based Image Retrieval Using Low Level Features of Automatically Extracted Regions of Interest," *Journal of Image and Graphics,,* vol. 1, no. 2, pp. 7-11, Mar. 2013.

[5] A. Suruliandi and G. Murugeswari, " Empirical Evaluation of LBP and its Derivates For Abnormality Detection In Mammogram Images," *Ictact Journal on Image and Video Proc,* vol. 4, no. 4, pp. 824-830, 2014.

[6] T. Ojala, M. Piettikainen, and T. Maenpaa, "Multiresolution gray-scale and rotation

invariant texture classification with local binary patterns," *IEEE Transactions on Pattern Analysis and Machine Intelligence,* vol. 24, no. 7, pp. 971-987, July 2002.

[7] F. Baji, M. Mocanu and D. Popa, "Detection the Mid-Sagittal Plane in Brain Slice MR Images by Using Local Ternary Pattern," in *2018 International Conference on Development and Application Systems (DAS) 14th Edition*, Suceava - Romania, May 24-26, 2018, DOI: 10.1109/DAAS.2018.8396086.

[8] A. Khokher and R. Talwar, " Content-based Image Retrieval: Feature Extraction Techniques and Applications," *International Journal of Computer Applications,* vol. 4, pp. 9-14, 2012.

[9] S. P. Mathew, V. E. Balas, K. Zachariah and P. Samuel, " A Content-based Image Retrieval System Based on Polar Raster Edge Sampling Signature," *Acta Polytechnica Hungarica,* vol. 11, no. 3, pp. 25-36, 2014.

[10] R. Chaudhari, and A. M. Patil, "Content Based Image Retrieval Using Color and Shape Features," *International Journal of Advanced Research in Electrical, Electronics and Instrumentation Engineering,* vol. 1, no. 5, pp. 386-392, 2012.

[11] A. Loredana, and S. Udristoiu, "Study of Medical Image Segmentation using a Statistical Framework," *ANNALS of the university of Craiova,* vol. 9, no. 36, pp. 65-70, 2012.

[12] X. Tan and B. Triggs, "Enhanced local texture feature sets for face recognition under difficult lighting conditions," in *IEEE Trans. Image Process*, pp. 1635–1650, 2010.

[13] D. Unay, A. Ekin and R. Jasinschi, "MEDICAL IMAGE SEARCH AND RETRIEVAL USING LOCAL BINARY PATTERNS AND KLT FEATURE POINTS," in *2008 15th IEEE International Conference on Image Processing*, San Diego, CA, USA, pp. 997-1000, Oct. 2008.

[14] F. Baji and M. Mocanu, "Uniform Extended Local Ternary Pattern for Content Based Image Retrieval," in *22nd International Conference on System Theory,Control and Computing, ICSTCC 2018*, Sinaia, Romania., 2018.

[15] S. Wan, H. Lee, J.G fujimoto, X. Huang and C. Zhou, " OCM image texture analysis for tissue classification," in *2014 IEEE 11th International Symposium on Biomedical Imaging (ISBI)*, Beijing, China, pp. 93-96, May 2014, .

[16] H. Freeman and A. Saghri, "Generalized chain codes for planar curves," in *In Proceedings of the 4th International Joint Conference on Pattern Recognition.*, Kyoto, Japan, 701-703, November 7-10 1978.

[17] S. Mark and S. A. Alberto, Feature Extraction and Image Processing; chapter 7, Newnes: Replika Press PVT Ltd., 2002.

[18] U. C. Maya and K. Meenakshy, " Brain Tumor Segmentation Using Asymmetry Based Histogram Thresholding And K-Means Clustering," *International Journal of Research in Engineering and Technology,* vol. 3, no. 15, pp. 62-65, 2014.

[19] S. Nadia and B. Souhir, "A developed system for melanoma diagnosis," *International Journal of Computer Vision and Signal Processing,* vol. 3, pp. 10-17, 2013.

[20] G. V. Tcheslavski, ", (2009). "Morphological Image Processing: Basic concept," *Spring ELEN 4304/5365 DIP,* 2009, available:http://ee.lamar.edu/gleb/dip/index.htm.

[21] H. A. Aslam, T. Ramashri and M.I.A. Ahsan, "A New Approach to Image Segmentation for Brain Tumor detection using Pillar K-means Algorithm," *International Journal of Advanced Research in Computer and Communication Engineering,* vol. 2, no. 3, pp. 1429-1436, 2013.

[22] P.J. Rousseeuw, "Silhouettes: a graphical aid to the interpretation and validation of cluster analysis," *Journal of Computational and Applied Mathematics,,* vol. 20, pp. 53-65, 1987.

[23] M. Kass, A. Witkin, and T. Terzopoulous, "Snakes: Active Contour Models," *international Journal of Computer Vision,* pp. 321-331, 1988.

[24] T. Boonnuk, S. Srisuk, and T. Sripramong, "Texture Segmentation Using Active Contour Model with Edge Flow Vector," *International Journal of Information and Electronics*

Engineering, vol. 5, no. 2, pp. 107-111, 2015.

[25] N. Otsu, " A Threshold Selection Method from Gray-Level Histograms," *IEEE Transactions On Systrems, Man, And Cybernetics,* Vols. SMC-9, no. 1, pp. 62-66, Jan. 2008.

[26] A. A. Mohamed, and R. V. Yampolskiy, "Adaptive Extended Local Ternary Pattern (AELTP) for Recognizing Avatar Faces," in *2012 11th International Conference on Machine Learning and Applications*, Boca Raton, FL, USA, pp. 57-62, Dec. 2012..

[27] L. Rocha, L. Velho, P. P. Carvalho, "Image Moments-Based Structuring and Tracking of Objects," in *Proc. of IEEE XV Brazilian Symposium on Computer Graphics and Image Processing*, DOI: 10.1109/SIBGRA.2002.1167130,ISBN: 0-7695-1846-X, Fortaleza-CE, Brazil, pp. 1-7, 2002.

[28] F. Baji and M. Mocanu, "Chain Code Approach for Shape based Image Retrieval," *Indian Journal of Science and Technology,* vol. 11, no. 3, pp. 1-17, Jan. 2018 DOI: 10.17485/ijst/2018/v11i3/119998.

[29] S. A. Jayasuriya and A. W. Liew, "Symmetry Plane Detection in Neuroimages based on Intensity Profile Analysis," in *International Symposium on Information Technology in Medicine and Education*, Hokkaido, Japa, 2012.

[30] F. Baji, M. Mocanu and D. Popa, "Brain Tumor Detection Based on Asymmetry and K-Means Clustering MRI Image Segmentation," *Journal of Engineering Science and Technology,* 2018.

[31] Y. Lium, R. T. Collins and W. E. Rothfus, " Automatic Extraction of the Central Symmetry (MidSagittal) Plane from Neuroradiology Images," The Robotics Institute, Carnegie Mellon University, 1996.

[32] A. Bianchi, J. V. Miller, E. T. Tan and A. Montillo, "Brain Tumor Segmentation With Symmetric Texture And Symmetric Intensity-Based Decision Forests," in *Proc. IEEE International Symp Biomed Imaging*, Buffalo, USA, 2013.

[33] M. Mokhomo, "Automatic Detection and Segmentation of Brain Lesions from 3D MR and CT Images," M.S. thesis, Faculty of Engineering, Cape Town University South Africa, 2014.

[34] S. R. Nilkamal and V.J. Shweta, "ABCD rule based automatic computer-aided skin cancer detection using MATLAB," *International Journal Computer Technology and Applications,* vol. 4, no. 4, pp. 691-697, 2013.

[35] F. Baji and M. Mocanu, "Diagnosis Melanoma Skin Cancer Using ABCD Rule, Statistic Texture Feature and Lesion Symptoms," *ANNALS of the University of Craiova,* vol. 13, no. 40, pp. 20-27, 2016.

[36] C. Sahil, J. Sonika and K. Bhavneet, " Content based Image Retrieval using Selective Region Matching with Region of Interest and SVM," *International Journal of Computer Applications,* vol. 137, pp. 28-33, 2016.

[37] W. Stolz, A. Riemann, A. B. Cognetta, L. pillet, et al, "ABCD rule of dermatoscopy: A new practical method for early recognition of malignant melanoma," *European Journal of Dermatology ,* vol. 4, p. 521–527, 1994.

[38] K. A. Johnson and J. Alex Becker , "the Whole Brain Atlas," 1999. [Online]. Available: "http://www.med.harvard.edu/AANLIB/home.html".

[39] F. Baji and M. Mocanu, "Performance Analysis of K-Means Clustering for Brain Tumor Detection," 2018.